The Nuclear Equation of State and Neutron Stars

J. M. Lattimer

Department of Physics & Astronomy

STONY BROOK UNIVERSITY

The Strong Interaction: From Quarks and Gluons to Nuclei and Stars
International School of Nuclear Physics 40th Course
Erice, Italy
16-24 September, 2018

Neutron Star Mass and Radius Measurements

- Constraints from GR, Causality and a Neutron Star Maximum Mass
- Nuclear theoretical and experimental constraints
- Photospheric Radius Expansion Bursts
- Quiescent Low-Mass X-ray Binaries
- Pulsar Timing
- NICER and Moment of Inertia Constraints
- GW170817

Neutron Star Radii and Nuclear Symmetry Energy

- Radii are highly correlated with neutron star matter pressure at $1-2n_s \simeq 0.16-0.32\ \mathrm{fm}^{-3}$.
- Neutron star matter is nearly pure neutrons, $x \sim 0.04$.
- Nuclear symmetry energy

$$S(n) \equiv E_0(n) - E_{1/2}(n)$$

$$E_x(n) \simeq E_{1/2}(n) + S_2(n)(1-2x)^2 + \ldots$$

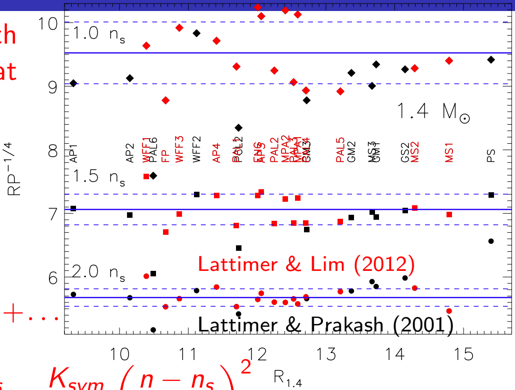

$$S(n) \simeq S_2(n) \simeq S_v + \frac{L}{3}\frac{n-n_s}{n_s} + \frac{K_{sym}}{18}\left(\frac{n-n_s}{n_s}\right)^2 \ldots$$

- $S_v \equiv S_2(n_s) \sim 32$ MeV, $L \sim 50$ MeV; nuclear systematics.
- Neutron matter energy and pressure at n_s:

$$E_0(n_s) \simeq S_v + E_{1/2}(n_s) = S_v - B \sim 13-17\ \mathrm{MeV}$$

$$p_0(n_s) = \left(n^2 \frac{\partial E_0(n)}{\partial n}\right)_{n_s} \simeq \frac{Ln_s}{3} \sim 2.1-3.7\ \mathrm{MeV\ fm}^{-3}$$

Causality + GR Limits and the Maximum Mass

A lower limit to the maximum mass sets a lower limit to the radius for a given mass.

Similarly, a precision upper limit to R sets an upper limit to the maximum mass.

$R_{1.4} > 8.15(10.9)$ km if $M_{max} \geq 2.01 M_\odot$.

$M_{max} < 3.0(2.3)\ M_\odot$ if $R < 13$ km.

$M - R$ curves for maximally compact EOS

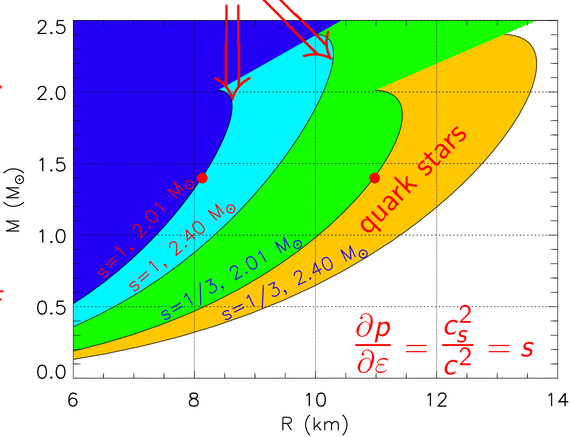

If quark matter exists in the interior, the minimum radii are substantially larger; maximum masses are considerably smaller.

Unitary Gas Bounds

Neutron matter energy should be larger than the unitary gas energy $E_{UG} = \xi_0 (3/5) E_F$

$$E_{UG} = 12.6 \left(\frac{n}{n_s}\right)^{2/3} \mathrm{MeV}$$

The unitary gas refers to fermions interacting via a pairwise short-range s-wave interaction with an infinite scattering length and zero range. Cold atom experiments show a universal behavior with the Bertsch parameter $\xi_0 \simeq 0.37$.

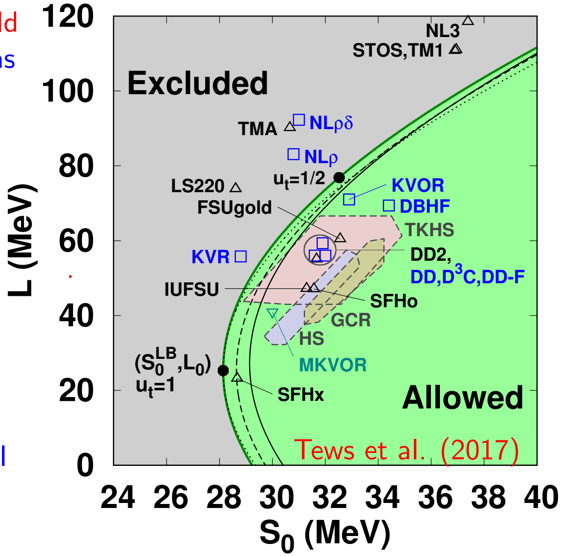

$S_v \geq 28.6$ MeV; $L \geq 25.3$ MeV; $p_0(n_s) \geq 1.35$ MeV fm^{-3}; $R_{1.4} \geq 9.7$ km

Theoretical and Experimental Constraints

H Chiral Lagrangian

G: Quantum Monte Carlo

neutron matter calculations from Hebeler et al. (2012)

unitary gas constraints from

Combined xperimental constraints are compatible with unitary gas bounds.

Neutron matter calculations are compatible with both.

$10.9\ \mathrm{km} \leq R_{1.4} \leq 13.1\ \mathrm{km}$

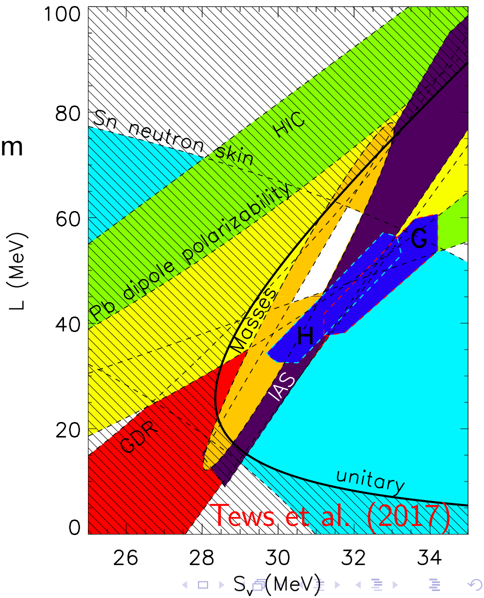

Predictions Using Piecewise Polytropes

Both the assumed minimum value of the neutron star maximum mass and the assumed matter pressure at $n_1 = 1.5 - 2n_s$ are important in restricting $M - R$ and $p - \varepsilon$ values.

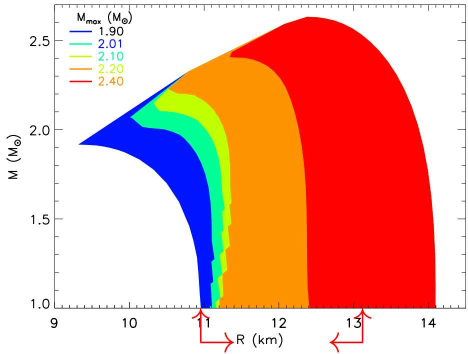

$8.4 < p_1 < 20$ MeV fm^{-3}

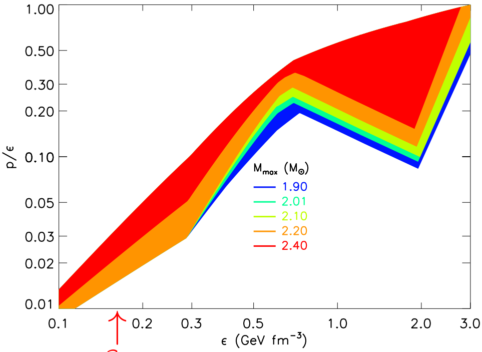

ε_s

Simultaneous Mass and Radius Measurements

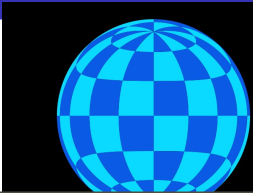

- Measurements of flux $F_\infty = (R_\infty/D)^2 \sigma T_{\rm eff}^4$ and color temperature $T_c \propto \lambda_{\rm max}^{-1}$ yield an apparent angular size (pseudo-BB):

$$R_\infty/D = (R/D)/\sqrt{1 - 2GM/Rc^2}$$

- Observational uncertainties include distance D, nonuniform T, interstellar absorption N_H, atmospheric composition

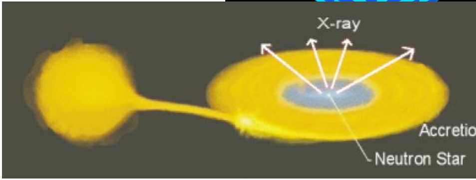

Best chances are:

  - Isolated neutron stars with parallax (atmosphere ??)
  - Quiescent low-mass X-ray binaries (QLMXBs) in globular clusters (reliable distances, low B H-atmospheres)
  - Bursting sources with peak fluxes close to Eddington limit (PREs); gravity balances radiation pressure

$$F_{\rm Edd} = \frac{cGM}{\kappa D^2}\sqrt{1 - 2GM/Rc^2}$$

Photospheric Radius Expansion X-Ray Bursts

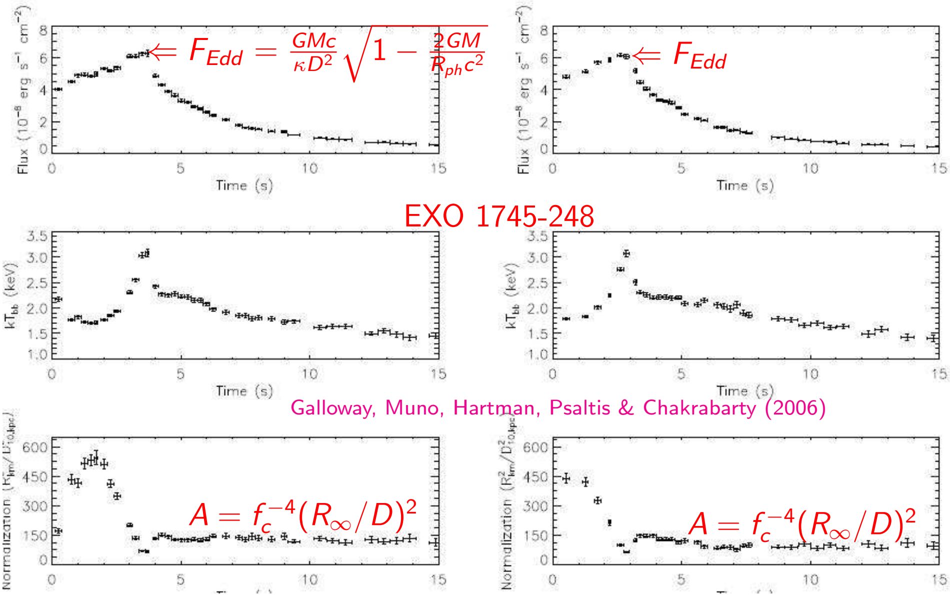

$$F_{Edd} = \frac{GMc}{\kappa D^2}\sqrt{1-\frac{2GM}{R_{ph}c^2}}$$

$\Leftarrow F_{Edd}$

EXO 1745-248

Galloway, Muno, Hartman, Psaltis & Chakrabarty (2006)

$$A = f_c^{-4}(R_\infty/D)^2$$

$$A = f_c^{-4}(R_\infty/D)^2$$

PRE Burst Models

Ozel et al. $z_{\rm ph} = z$ $\beta = GM/Rc^2$

$$
\begin{aligned}
F_{\rm Edd} &= \frac{GMc}{\kappa D}\sqrt{1-2\beta} \\
A &= \frac{F_\infty}{\sigma T_\infty^4} = f_c^{-4}\left(\frac{R_\infty}{D}\right)^2 \\
\alpha &= \frac{F_{\rm Edd}}{\sqrt{A}}\frac{\kappa D}{F_c^2 c^3} = \beta(1-2\beta) \\
\gamma &= \frac{A f_c^4 c^3}{\kappa F_{\rm Edd}} = \frac{R_\infty}{\alpha} \\
\beta &= \frac{1}{4} \pm \frac{1}{4}\sqrt{1-8\alpha} \\
\alpha &\le \frac{1}{8} \text{ required.}
\end{aligned}
$$

Steiner et al. $z_{\rm ph} << z$

$$
\begin{aligned}
F_{\rm Edd} &= \frac{GMc}{\kappa D} \\
\alpha &= \beta\sqrt{1-2\beta} \\
\theta &= \cos^{-1}\left(1-54\alpha^2\right) \\
\beta &= \frac{1}{6}\left[1+\sqrt{3}\sin\left(\frac{\theta}{3}\right)\right. \\
&\quad \left. -\cos\left(\frac{\theta}{3}\right)\right] \\
\alpha &\le \sqrt{\frac{1}{27}} \simeq 0.192 \text{ required.}
\end{aligned}
$$

EXO1745-248	4U1608-522	4U1820-30	KS1731-260	SAXJ1748.9-2021
0.19 ± 0.04	0.25 ± 0.06	0.24 ± 0.04	0.20 ± 0.03	0.18 ± 0.04

observed α values (Ozel et al.)

PRE $M - R$ Estimates

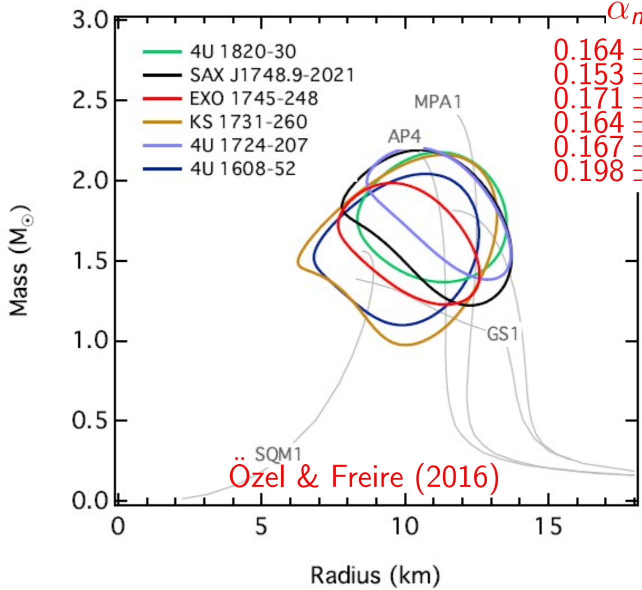

α_{min}

0.164 ± 0.024
0.153 ± 0.039
0.171 ± 0.042
0.164 ± 0.037
0.167 ± 0.045
0.198 ± 0.047

Özel & Freire (2016)

QLMXBs (Guillot & Rutledge 2013)

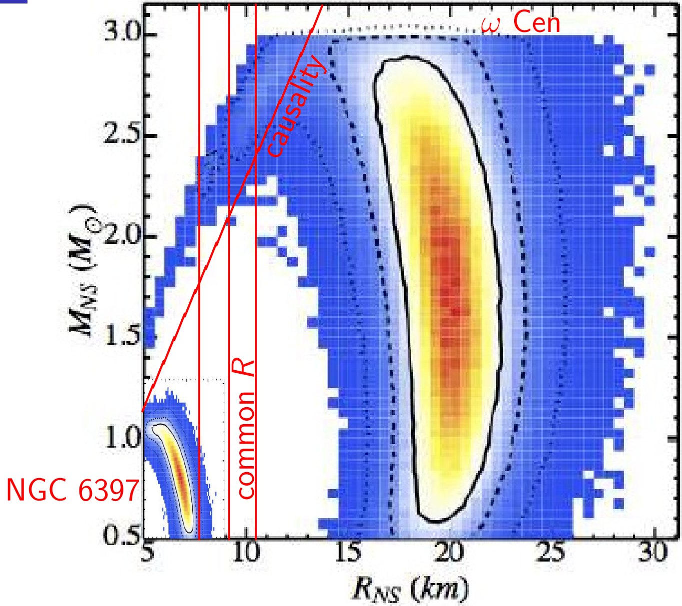

Guillot & Rutledge (

Reconciling sources with disparate values of R_∞, with little information concerning z, forces a solution near the smallest R_∞. Sources then have a wide range of predicted masses.

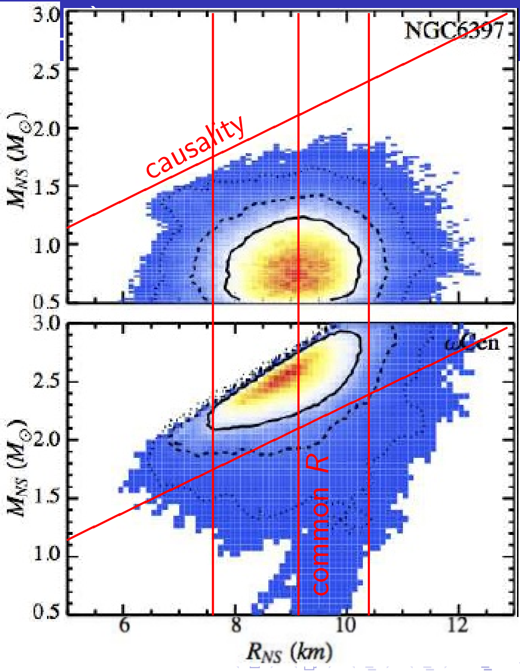

QLMXB $M - R$ Estimates

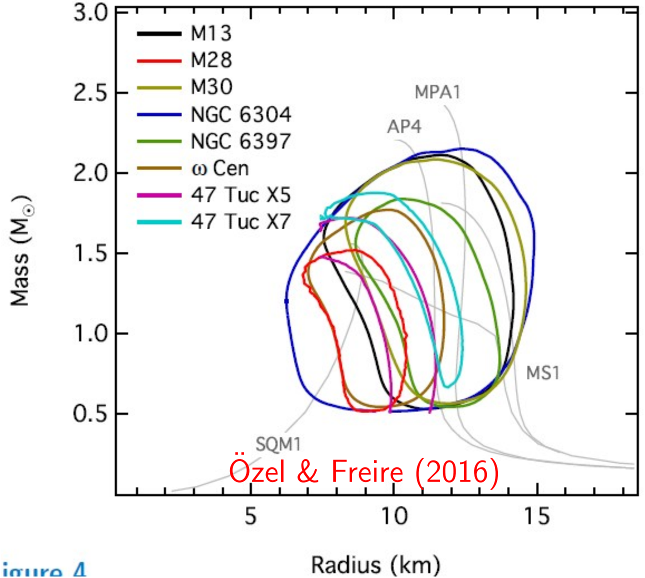

M13 QLMXB (Shaw et al. 2018)

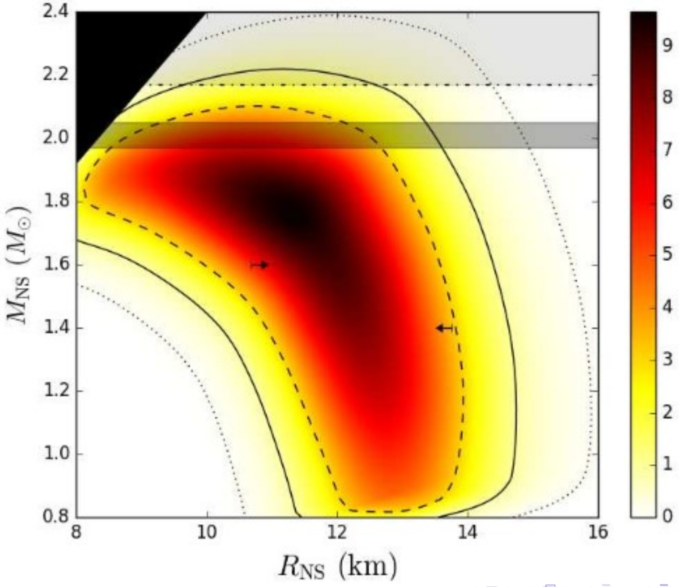

8 QLMXBs (Steiner et al. 2018)

Parameterized EOS priors

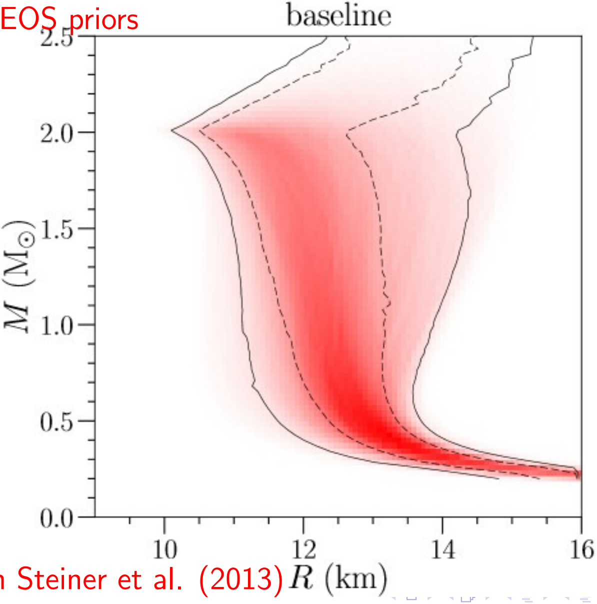

Consistent with Steiner et al. (2013)

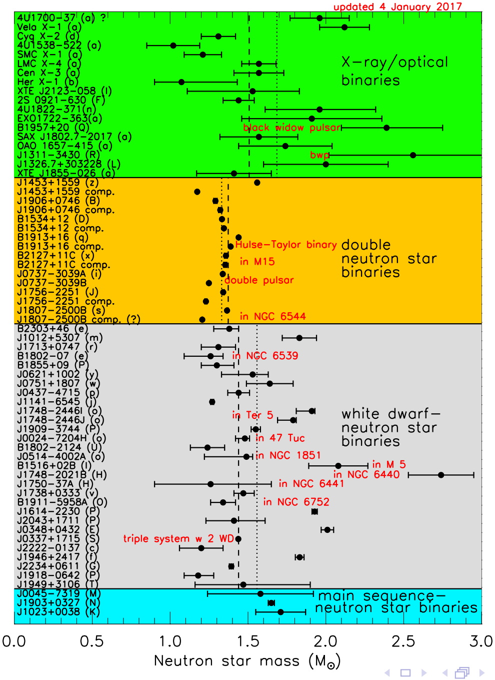

vanKerkwijk 2010

Romani et al. 2012

Although simple average mass of w.d. companions is 0.23 $M_\odot$ larger, weighted average is 0.04 $M_\odot$ smaller

Demorest et al. 2010
Fonseca et al. 2016
Antoniadis et al. 2013
Barr et al. 2016

Champion et al. 2008

Black Widow Pulsar PSR B1957+20

A 1.6ms pulsar in circular 9.17h orbit with $\sim 0.03\ M_\odot$ companion.
The pulsar is eclipsed for 50-60 minutes each orbit; eclipsing object has a volume much larger than the secondary or its Roche lobe.
Pulsar is ablating the companion leading to mass loss and the eclipsing plasma. The secondary may nearly fill its Roche lobe.
Ablation by the pulsar leads to secondary's eventual disappearance.
The optical light curve tracks the motion of the secondary's irradiated hot spot rather than its center of mass motion.

pulsar radial velocity

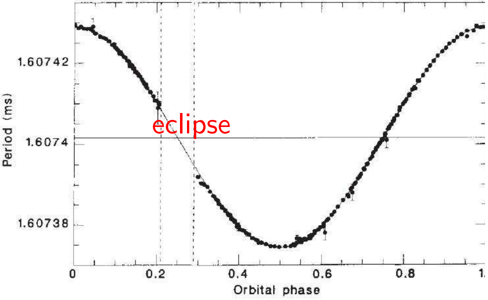

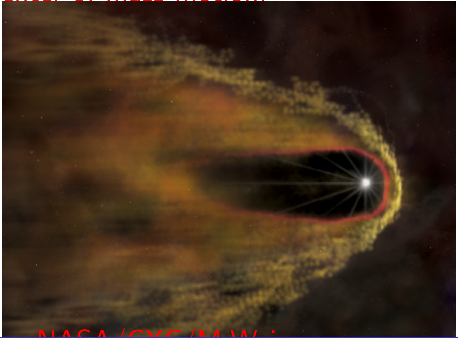

PSR J2215-5135

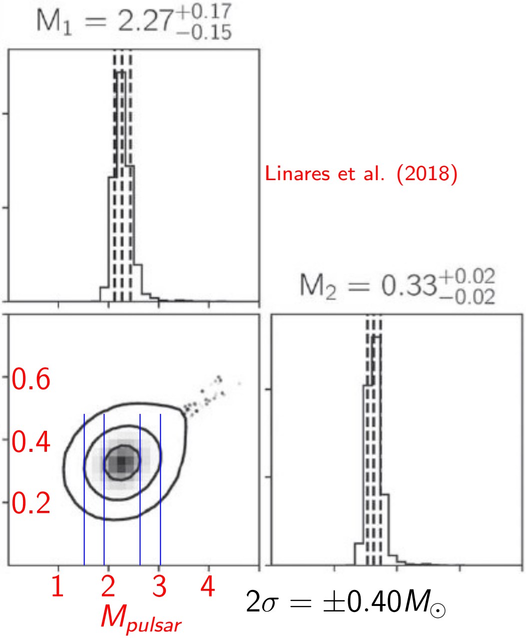

Linares et al. (2018)

- Redback binary MSP
- $P_{orb} = 4.14$ hr
- $T_{night} = 5660^{+260}_{-380}$ K
- $T_{day} = 8080^{+470}_{-280}$ K
- $D = 2.9 \pm 0.1$ kpc
- $e = 0.144 \pm 0.002$
- Roche lobe filling factor $f = 0.95 \pm 0.01$
- $M_{pulsar} = 2.27^{+0.17}_{-0.15} M_\odot$
- $M_{comp} = 0.33^{+0.02}_{-0.02} M_\odot$

$2\sigma = \pm 0.40 M_\odot$

Science Measurements

Reveal stellar structure through lightcurve modeling, long-term timing, and pulsation searches

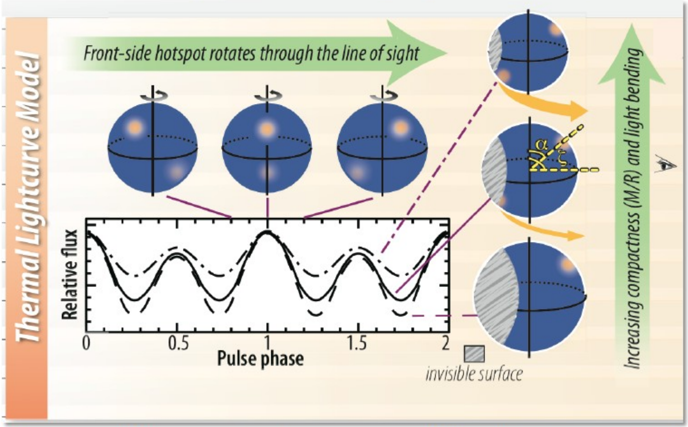

Lightcurve modeling constrains the compactness (M/R) and viewing geometry of a non-accreting millisecond pulsar through the depth of modulation and harmonic content of emission from rotating hot-spots, thanks to gravitational light-bending…

Science Measurements (cont.)

NICER

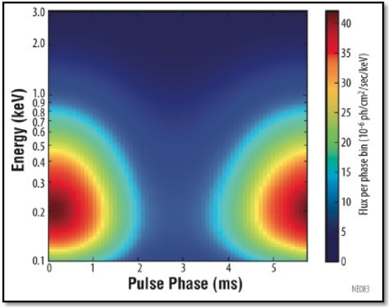

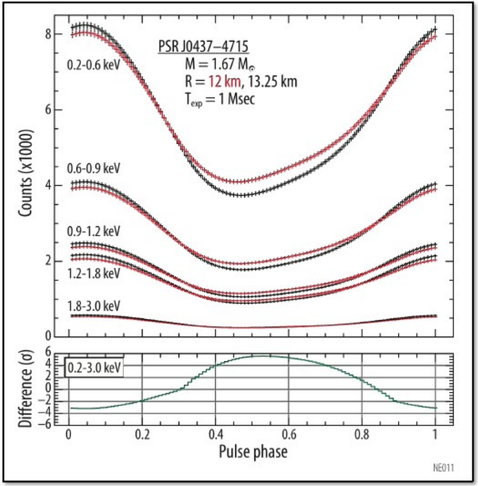

… while phase-resolved spectroscopy promises a direct constraint of radius *R*.

GW170817

- LIGO-Virgo detected a signal consistent with a BNS merger, followed 1.7 s later by a weak sGRB.
- 16600 orbits observed over 165 s.
- $\mathcal{M}_{\rm chirp} = 1.1867 \pm 0.0001\ M_\odot$
- $M_{\rm tot,max} = 2^{6/5}\mathcal{M}_{\rm chirp} = 2.726 M_\odot$
- $E_{\rm rad} > 0.025 M_\odot c^2$
- $D_L = 40 \pm 10$ Mpc
- $84 < \tilde{\Lambda} < 640$ (90%)
- $M_{\rm ejecta} \sim 0.06 \pm 0.02\ M_\odot$
- Blue ejecta: $\sim 0.01 M_\odot$
- Red ejecta: $\sim 0.05 M_\odot$
- Likely r-process production

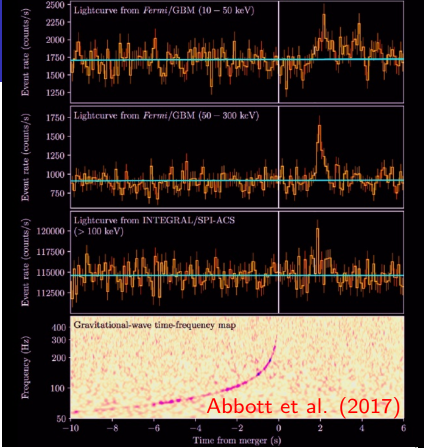

Abbott et al. (2017)

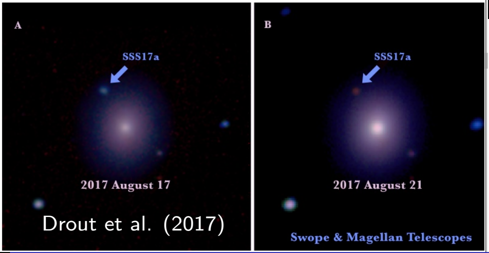

Drout et al. (2017)

DNS with only an upper limit to m_p

DNS with $\tau_{GW} = \infty$

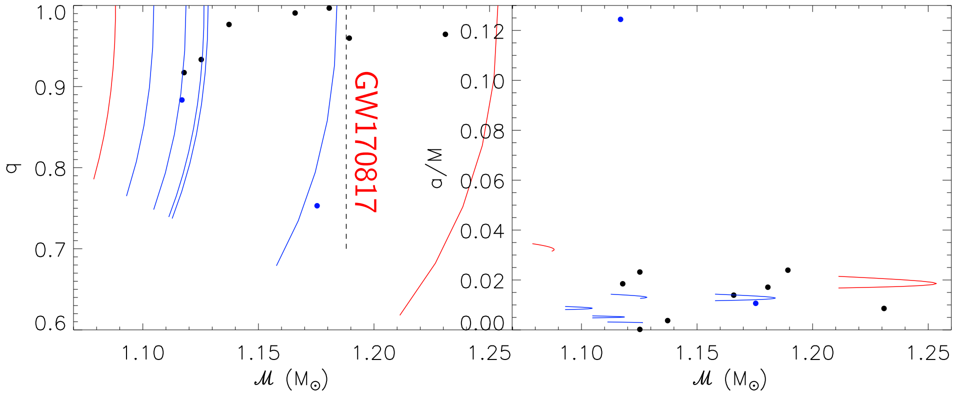

Waveform Model Parameter Determinations

There are 13 free wave-form parameters including finite-size effects at third PN order $(v/c)^6$. LV17 used a 13-parameter model; De et al. (2018) used a 9-parameter model.

- Sky location (2) EM data
- Distance (1) EM data
- Inclination (1)
- Coalescence time (1)
- Coalescence phase (1)
- Polarization (1)

Extrinsic

- Component masses (2)
- Perpindicular spins (2)
- Tidal deformabilities (2) correlated with masses

Intrinsic

Tidal Deformability

Tidal deformability λ is the ratio between the induced dipole moment Q_{ij} and the external tidal field E_{ij}, $Q_{ij} \equiv -\lambda E_{ij}$.

k_2 is the dimensionless Love number. It is convenient to work with the dimensionless quantity

$$\Lambda = \frac{\lambda c^{10}}{G^4 M^5} \equiv \frac{2}{3} k_2 \left(\frac{Rc^2}{GM}\right)^5 .$$

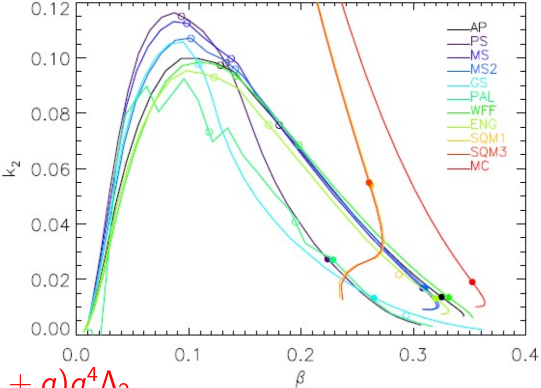

For a binary neutron star, the relevant quantity is

$$\bar{\Lambda} = \frac{16}{13} \frac{(1+12q)\Lambda_1 + (12+q)q^4\Lambda_2}{(1+q)^5}, \qquad q = M_2/M_1 \le 1$$

$$\delta\Phi_t = -\frac{117}{256} \frac{(1+q)^4}{q^2} \left(\frac{\pi f_{GW} G\mathcal{M}}{c^3}\right)^{5/3} \bar{\Lambda} + \cdots .$$

Deformability and the Radius

- $\Lambda = a(Rc^2/GM)^6$
  $a = 0.0085 \pm 0.0010$ for
  $M = 1.35 \pm 0.25\ M_\odot$

$$\tilde{\Lambda} = \frac{16}{13}\frac{(1+12q)\Lambda_1 + q^4(12+q)\Lambda_2}{(1+q)^5}$$

- $R_1 \simeq R_2 \simeq \hat{R}$

$$\tilde{\Lambda} \simeq \frac{16a}{13}\left(\frac{\hat{R}c^2}{G\mathcal{M}}\right)^6 \frac{q^{8/5}(12-11q+12q^2)}{(1+q)^{26/5}}$$

- $\tilde{\Lambda} = a'(\hat{R}c^2/G\mathcal{M})^6$
  $a' = 0.0035 \pm 0.0007$ for
  $\mathcal{M} = 1.2 \pm 0.2\ M_\odot$
  $a' = 0.0039 \pm 0.0002$ GW10817

- $\hat{R} = 11.5 \pm 0.3\ \frac{\mathcal{M}}{M_\odot}\left(\frac{\tilde{\Lambda}}{800}\right)^{1/6}$ km
  $\hat{R} = 13.4 \pm 0.1\ (\tilde{\Lambda}/800)^{1/6}$ km GW170817

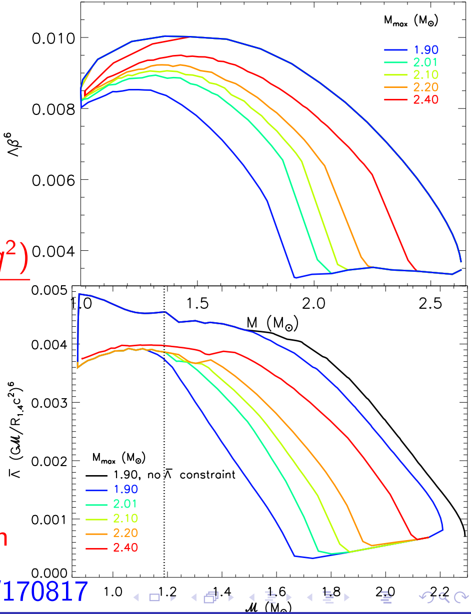

Tidal Deformabilities

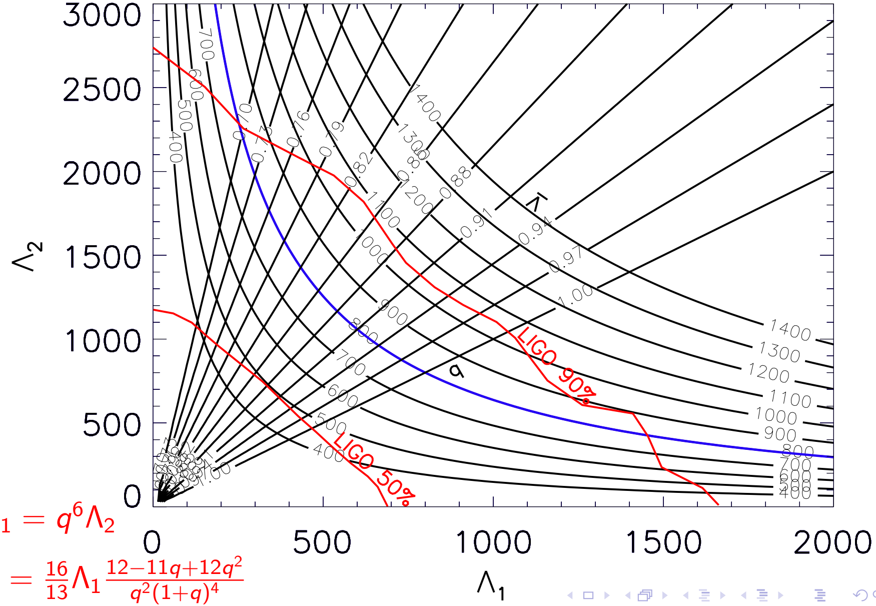

$\Lambda_1 = q^6 \Lambda_2$

$\tilde{\Lambda} = \frac{16}{13}\Lambda_1 \frac{12-11q+12q^2}{q^2(1+q)^4}$

Measurability of Tidal Deformability

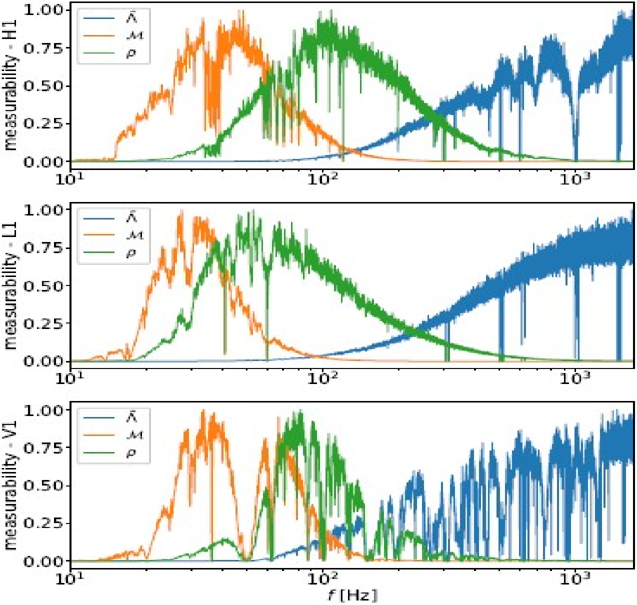

De et al. (2018)

A Re-Analysis of GW170817, De et al. (2018)

- De18 takes advantage of the precisely-known electro-magnetic source position (Soares-Santos et al., 2017).
- Uses existing knowledge of the H_0 and the redshift of NGC 4993 to fix the distance (Cantiello et al., 2017).
- Assumes both neutron stars have the same equation of state, which impliies $\Lambda_1 \simeq q^6 \Lambda_2$.
- Baseline model effectively has 9 instead of 13 parameters.
- Explores variations of mass, spin and deformability priors.
- Low-frequency cutoff taken to be 20 Hz, not 30 Hz (LV17), doubling the number of analyzed orbits.
- De18 finds mild evidence ($\mathcal{B} \sim 10$) for finite-size effects, but no evidence for spins.
- Finds a 90% lower confidence bound to $\tilde{\Lambda}$.
- Finds strong evidence ($\mathcal{B} \sim 400$) for a common EOS, which argues against one star being a hybrid star.
- Finds including $\Lambda - M$ correlations reduces $\tilde{\Lambda}$ by $\sim 30\%$.

GW170817

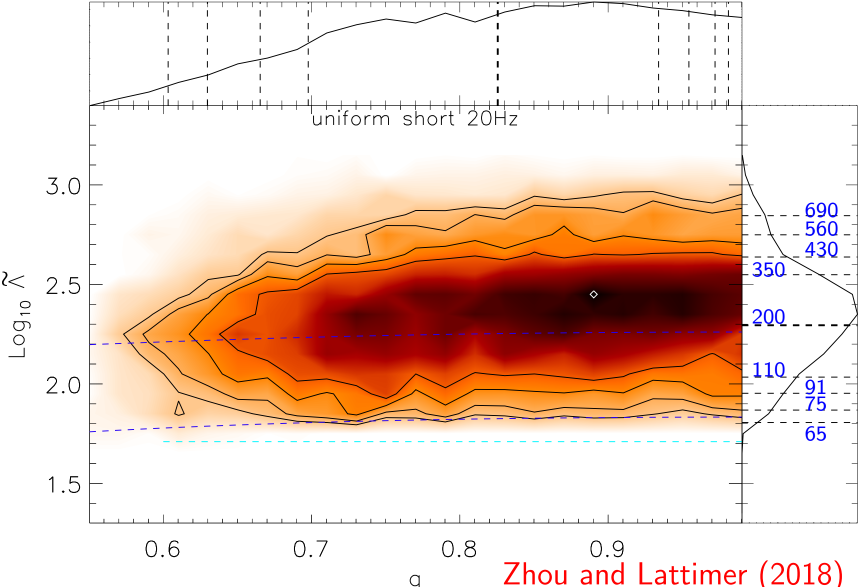

Zhou and Lattimer (2018)

GW170817

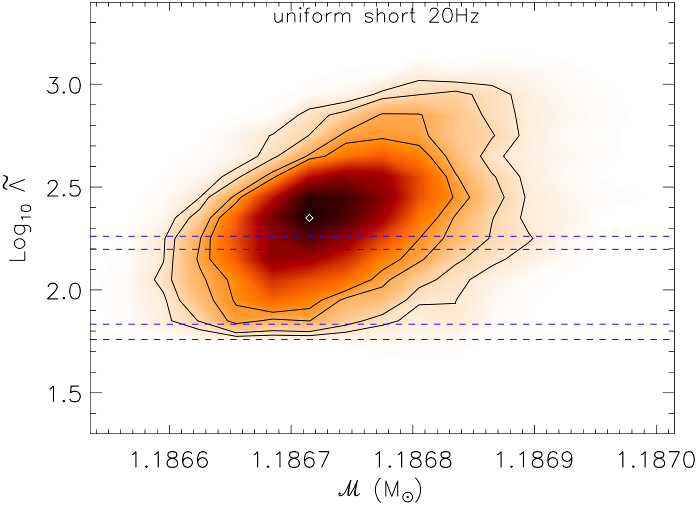

Zhou and Lattimer (2018)

GW170817

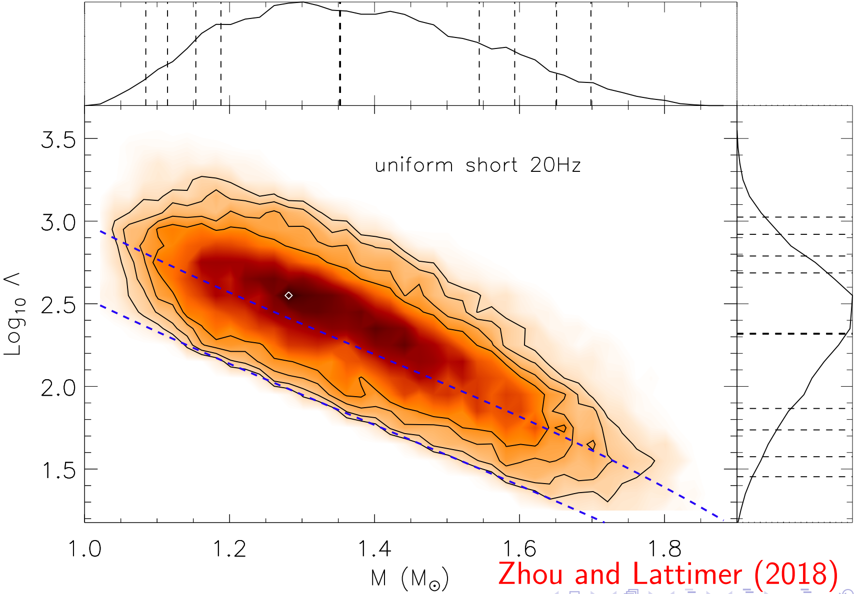

Zhou and Lattimer (2018)

GW170817

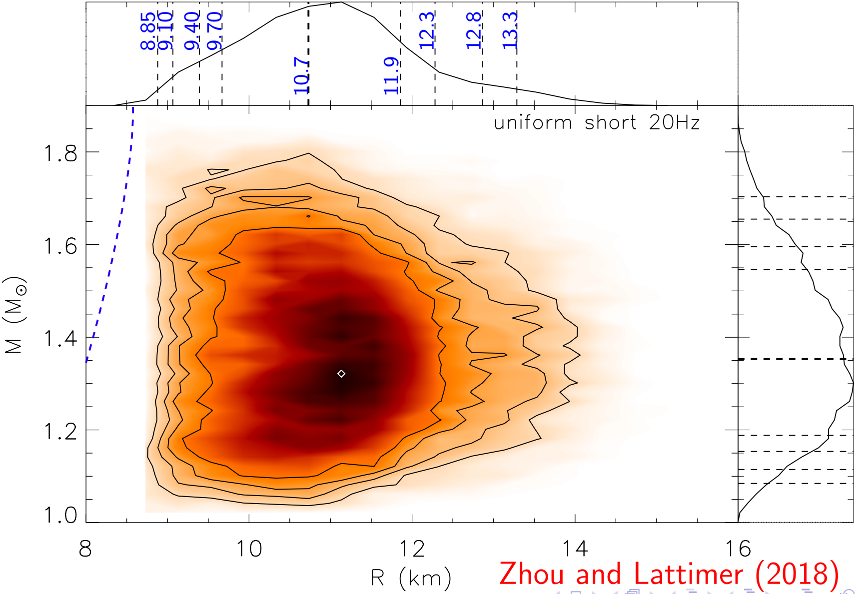

Zhou and Lattimer (2018)

LV18 Determined $R_1 \simeq R_2$ for GW170817

$\Lambda_2 - \Lambda_1$ correlations from parameterized EOSs with $M_{max} > 1.97 M_\odot$

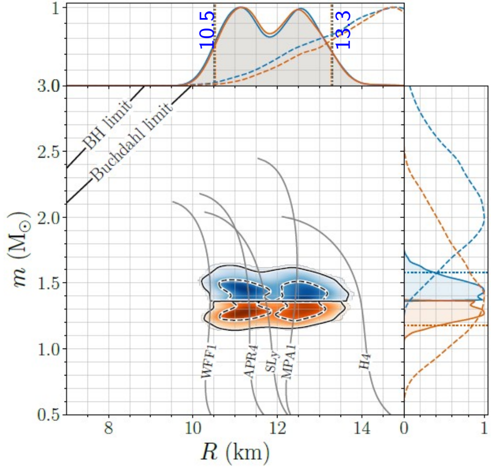

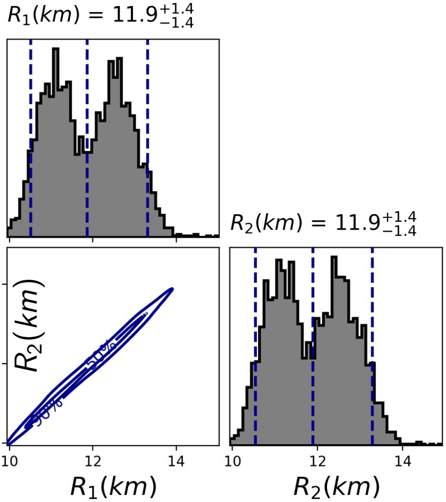

LV18

GW170817 Summary

- It's important to include correlations among $\Lambda_1, \Lambda_2, M_1$ and M_2 in a model-independent fashion.
- It's important to include as many orbits as possible; low frequency cutoff is about 20 Hz.
- Better waveform models appear to reduce fitting uncertainties in $\tilde{\Lambda}$ (by about 15%).
- LV18 constraints on radii depend on how the EOS is modeled. Compared to using bounds on the deformability-mass correlation, their method biases results towards central values of the EOS parameter and radius ranges.
- Upper bounds to M_{max} should not play a role in radius determinations, but do in the LV18 analyses.
- With a better waveform model, De et al. should obtain a 90% confidence upper limit to $\hat{R}$ of about 12.4 km.
- With unitary gas constraint, $\tilde{\Lambda} > 160$, $\hat{R} > 10.7$ km.
- Coughlin et al. (2018) claim $\tilde{\Lambda} > 197$ from EM evidence.

The Future

- A few more neutron star mergers per year should allow significant improvements to radii and maximum mass constraints. The systems are expected to be quite similar to GW170817, except they will be further away and may not have optical transients or sGRBs.
- It should be possible to establish a pulsar-timing bounds to the moment of inertia of PSR 0737-3037A, which with its known mass, will set tight radius constraints.
- NICER expects to release radius estimates with 1 km-accuracy by years' end.
- Ongoing and planned nuclear experiments, including neutron skin measurements at J-Lab and Mainz, will offer competing information.
- Further *ab-initio* improvements will be important.
- Further measurements of black widow pulsar systems should give us some surprises.